



RESEARCH LETTER

10.1002/2015GL067550

Key Points:

- Anomalous surface-intensified warming in the Southern California Current System during 2014–2015
- Depressed thermocline, high stratification, freshening, and deepening of chl *a* fluorescence maximum
- Local anomalous atmospheric forcing caused the unusual oceanic conditions

Correspondence to:

K. D. Zaba,
kzaba@ucsd.edu

Citation:

Zaba, K. D., and D. L. Rudnick (2016), The 2014–2015 warming anomaly in the Southern California Current System observed by underwater gliders, *Geophys. Res. Lett.*, 43, 1241–1248, doi:10.1002/2015GL067550.

Received 23 DEC 2015

Accepted 16 JAN 2016

Accepted article online 20 JAN 2016

Published online 13 FEB 2016

The 2014–2015 warming anomaly in the Southern California Current System observed by underwater gliders

Katherine D. Zaba¹ and Daniel L. Rudnick¹¹Scripps Institution of Oceanography, La Jolla, California, USA

Abstract Large-scale patterns of positive temperature anomalies persisted throughout the surface waters of the North Pacific Ocean during 2014–2015. In the Southern California Current System, measurements by our sustained network of underwater gliders reveal the coastal effects of the recent warming. Regional upper ocean temperature anomalies were greatest since the initiation of the glider network in 2006. Additional observed physical anomalies included a depressed thermocline, high stratification, and freshening; induced biological consequences included changes in the vertical distribution of chlorophyll fluorescence. Contemporaneous surface heat flux and wind strength perturbations suggest that local anomalous atmospheric forcing caused the unusual oceanic conditions.

1. Introduction

An ongoing large-scale warming event has persisted in the eastern North Pacific basin from late 2013 to present. Positive sea surface temperature (SST) anomalies were observed from Alaska to Mexico, though the timing and strength of multiple warm patches varied along the west coast of North America. As the unique event is still unfolding, anecdotal reports of abnormal ocean properties, weather patterns, and ecosystem disturbances are abundant; however, relevant scientific literature is just beginning to appear and lacks a full explanation of the unfamiliar phenomenon. The warming was initially recognized in the south central region of the Gulf of Alaska, where positive SST anomalies were linked to a high sea level pressure (SLP) system [Wang *et al.*, 2014] that altered westerly winds [Whitney, 2015] and, consequently, reduced cooling by horizontal advection and air-sea heat exchange [Bond *et al.*, 2015]. Throughout other areas of the basin, a comprehensive understanding of the causes, consequences, and connectivity of regional anomalies remain to be determined.

This report provides a first assessment of the appearance and evolution of coastal anomalies in the Southern California Current System (SCCS), which constitutes the biologically productive eastern boundary of the North Pacific subtropical gyre and was amongst the various regions affected by the recent warming. In the SCCS, surface-intensified temperature anomalies began in early 2014 and reached maximum excursions during the winter of 2014–2015. Concurrent hydrographic anomalies included depressed isopycnals, high stratification, and freshening. Changes in the vertical structure of chlorophyll *a* (chl *a*) fluorescence reveal potential ecological impacts. Local atmospheric anomalies are shown to be the main cause of the recent SCCS warming.

In general, the coupled effects of local surface heat flux [Winant and Dorman, 1997; Beardsley *et al.*, 1998], wind stress [Nelson, 1977], horizontal advection [Bograd *et al.*, 2001], and upwelling strength [Huyer, 1983] regulate the physical and biological properties of the California Current System (CCS), including heat content. Interannual variability of these physical processes is modulated by low-frequency climatic processes such as El Niño–Southern Oscillation (ENSO) [McPhaden, 1999; Lynn and Bograd, 2002; Schwing *et al.*, 2002], the Pacific Decadal Oscillation [Mantua *et al.*, 1997], the North Pacific Gyre Oscillation [Di Lorenzo *et al.*, 2008], and decadal stratification changes [Roemmich and McGowan, 1995; Bograd and Lynn, 2003]. Though the ongoing 2014–2015 warming appears different from the familiar patterns of climate variability, we consider the forcing mechanisms that govern interannual variability on the same timescales as ENSO.

For instance, equatorial El Niño events induce remote midlatitude effects by several mechanisms: atmospheric teleconnections that alter wind patterns [Emery and Hamilton, 1985; Alexander *et al.*, 2002; Schwing *et al.*, 2002; Todd *et al.*, 2011a], poleward propagation of coastally trapped waves that deepen the thermocline [Chelton and Davis, 1982; Ramp *et al.*, 1997; Meyers *et al.*, 1998], and anomalous northward advection of warm, southerly

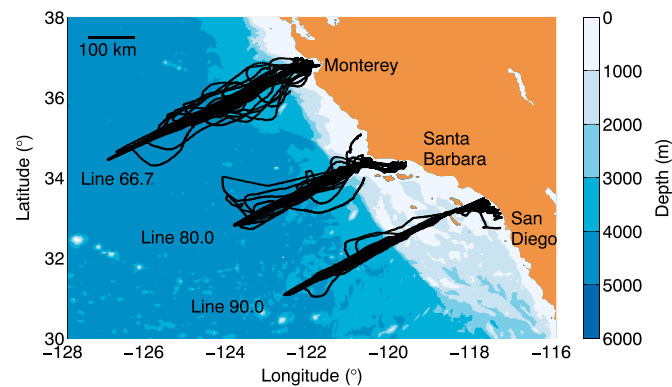


Figure 1. Glider profile locations from October 2006 to June 2015 along CalCOFI lines 66.7, 80, and 90 in black. Blue and tan contours show bathymetry and land, respectively.

CCS region. Unrelated to El Niño, increased downward heat flux from the atmosphere into the ocean has been shown to induce long-term positive SST and stratification trends [Miller *et al.*, 1994; Di Lorenzo *et al.*, 2005]. Each of these processes is considered in our subsequent analysis of recent oceanic anomalies in the SCCS.

2. Methods

The California Underwater Glider Network was established in order to monitor the regional effects of large-scale climate variability [Davis *et al.*, 2008]. Subsurface observations are obtained by Spray gliders [Sherman *et al.*, 2001; Rudnick *et al.*, 2004] continuously repeating sections that extend 350–500 km offshore along California Cooperative Oceanic Fisheries Investigations (CalCOFI) lines 66.7, 80, and 90 (Figure 1). Following a sawtooth trajectory, the buoyancy-driven autonomous underwater vehicles dive to 500 m and measure ocean parameters during the ascent. The glider network provides good spatial and temporal resolution as each dive cycle occurs over 3 h and 3 km, approximately, and each section takes 2–3 weeks to occupy. This analysis incorporates glider-measured pressure, temperature, salinity, velocity, and chl *a* fluorescence from October 2006 to June 2015.

We use an objective analysis [Bretherton *et al.*, 1976] to map the temperature, salinity, and velocity data to evenly spaced three-dimensional grids, which have a resolution of 10 m in depth, 5 km in along-line distance, and 10 days in time. Glider data are averaged to 10 m depth bins; then two-dimensional maps, in distance and in time, are computed for each discrete depth level. Our choice of decorrelation length and timescales, 30 km and 60 days, in the mapping algorithm acts to filter the data by removing the high-frequency, small-scale variability, like that of internal waves [Rudnick and Cole, 2011]. The resulting maps contain only low frequency, large-scale variability, the scales of interest when analyzing interannual cycles. All anomalies are defined relative to a mean annual cycle from 2007 to 2013.

Ancillary data products include the Oceanic Niño Index (ONI) and the National Centers for Environmental Prediction North American Mesoscale (NAM) model. Provided by the NOAA Climate Prediction Center, the ONI is defined as the SST anomaly averaged over the Niño 3.4 region (5°S–5°N, 120°–170°W) and smoothed with a 3 month running mean. The equatorial SST anomalies are relative to a 1981–2000 base period. The NAM model, from which we obtain surface heat flux and wind fields, is accessed via the NOAA National Operational Model Archive and Distribution System. In our analysis, we spatially average the atmospheric anomalies over the entire California Underwater Glider Network domain of Figure 1 ([–128°, –116°W] × [30°, 38°N]), including only the data points over the ocean and excluding those over land. For consistency with the glider-derived oceanic anomalies, NAM monthly surface forcing anomalies are defined relative to means over 2007–2013.

3. Results

3.1. Oceanic Conditions

Surface waters in the SCCS exhibited a striking temperature increase during 2014–2015 (Figure 2). The duration and amplitude of the warming signal were unprecedented since the initiation of the California Underwater Glider Network in October 2006. The anomalously warm waters were generally confined to

water masses [Bograd *et al.*, 2001; Lynn and Bograd, 2002]. The poleward wind anomalies and coastally trapped waves cause downwelling anomalies that suppress the upward flux of cool, deep waters, effectively warming the upper ocean. Mean regional circulation is composed of the southward California Current [Lynn and Simpson, 1987] and the northward California Undercurrent [Lynn and Simpson, 1990; Todd *et al.*, 2011b], which advect cool, fresh and warm, salty water into the region, respectively. Unseasonable strengthening of heat transport by the California Undercurrent can warm the

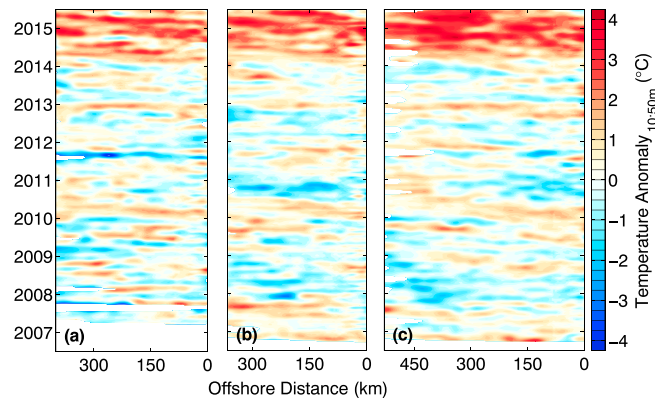


Figure 2. Hovmöller plots of temperature anomalies depth averaged over 10–50 m along (a) line 66.7, (b) line 80, and (c) line 90. A striking upper ocean temperature anomaly began in early 2014 and remained through mid-2015.

than the distance between lines, such as regional wind stress [Chelton *et al.*, 2004] and cloud cover [Iacobellis and Cayan, 2013], govern surface temperature fluctuations. The remarkably correlated rise of nearshore temperature anomalies in early 2014 suggests a large-scale control of shallow oceanic temperatures that synchronously affected the west coast of Southern and Central California.

In addition to its above average temperatures, the surface layer capping the water column was characterized by high static stability. Beginning in late spring of 2014, the squared buoyancy frequency anomaly averaged over 10–50 m depth was positive (Figure 4b), caused by the presence of anomalously warm, stratified, low-density surface water above the thermocline. Stratification strengthening acts to limit vertical fluxes of upwelled properties, thereby acting as a barrier and inhibiting the input of cool deep water to the surface layer [Roemmich and McGowan, 1995; Bograd and Lynn, 2003].

Downwelling anomalies persisted during 2014–2015, causing a downward shift of various depth-dependent properties. Characteristic of eastern boundary currents, upwelling in the CCS maintains isopycnal shoaling toward the coast [Huyer, 1983] and a downwelling anomaly corresponds with a deepening of isopycnals, isotherms, and isohalines, relative to mean conditions. The 26.0 kg/m³ isopycnal, typically found within the thermocline [Todd *et al.*, 2011a], was anomalously deep along all three glider lines (Figure 4c). A depressed thermocline vertically displaces warm, fresh water downward, causing both warming at the thermocline (Figure 3a) and freshening at the halocline (Figure 3b). Figure 3 displays depth-dependent temperature and salinity anomalies along line 90; the subsurface patterns along lines 66.7 and 80 (not shown) are similar. The surface intensification of the positive temperature anomalies (Figure 3a) suggests that in addition to the subsurface warming at the thermocline

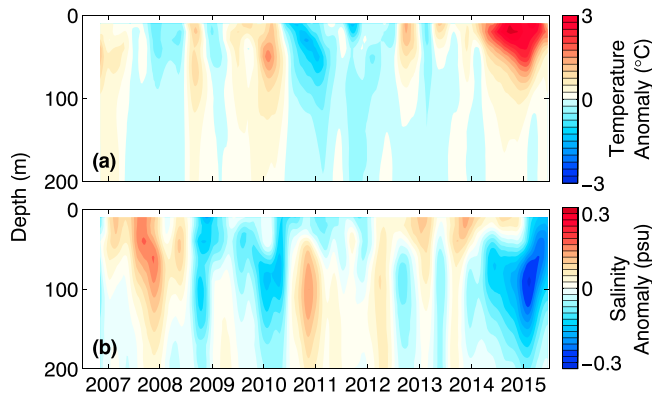


Figure 3. Depth-dependent (a) temperature and (b) salinity anomalies averaged over the inshore 200 km along line 90 and filtered with a 3 month running mean. A surface-intensified warming and a subsurface freshening persisted during 2014–2015.

the upper 50 m, below which temperature variability was weak (Figure 3a). Maximum temperature anomalies reached 4.5°C along line 66.7 and 5°C along lines 80 and 90.

The warming occurred simultaneously along all three glider lines (Figures 2 and 4a). Nearshore temperature anomalies appeared in early 2014, reached extremes in late 2014, and remained positive for over 18 months through the end of the analysis period in June 2015 (Figure 4a). Within the extended glider record, we typically find that spatially heterogeneous atmospheric processes of smaller scale

depth (approximately 50 m), there was anomalous oceanic heat gain at the air-sea interface. Maximum freshening occurred around 90 m (Figure 3b), the climatological depth of the halocline. The observed downwelling anomalies indicate that there was reduced upward transport of cold, saline water to the surface, causing cooling of the mixed layer by vertical advection during 2014–2015 to be less effective than normal.

The influence of anomalous horizontal advection on nearshore properties is apparent, though it does not have a warming effect. To address horizontal advection, we analyzed along-isopycnal variability and alongshore velocity.

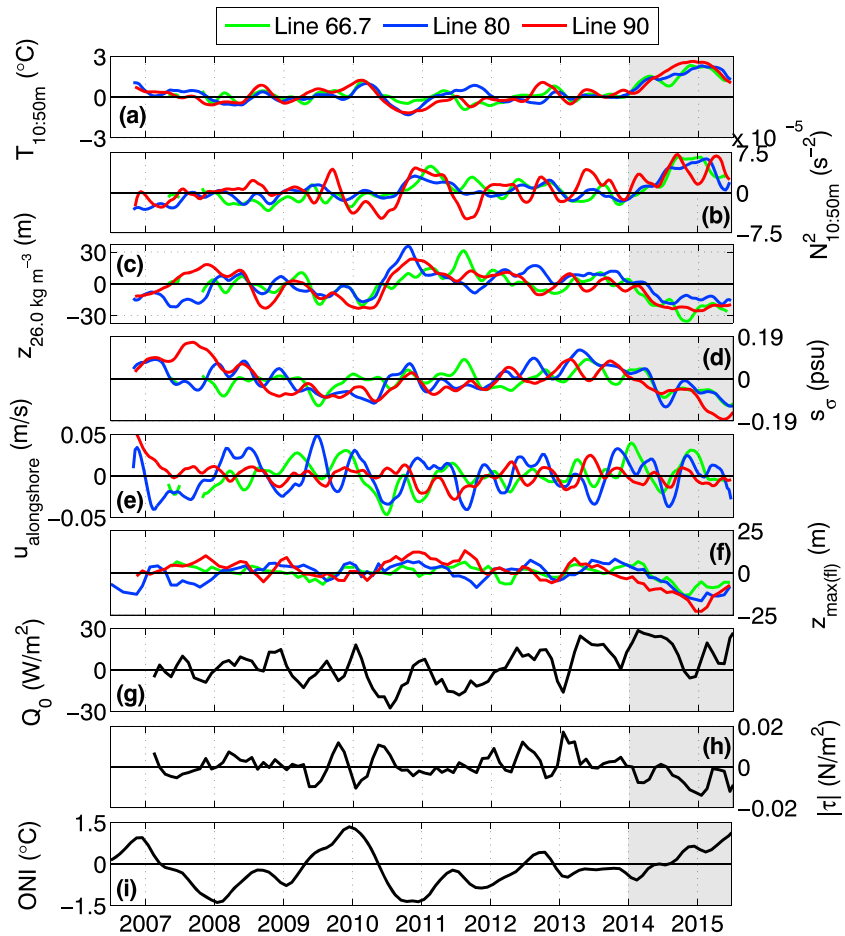


Figure 4. Time series of oceanic and atmospheric property anomalies. Glider-measured (a) temperature in the upper 50 m, (b) buoyancy frequency squared in the upper 50 m, (c) depth of the 26.0 kg/m³ isopycnal (negative indicates deep), (d) salinity along isopycnals (the 25.75, 25.50, and 25.25 kg/m³ isopycnals for lines 66.7, 80, and 90, respectively), (e) alongshore velocity depth averaged over the upper 500 m, and (f) depth of the subsurface fluorescence maximum (negative indicates deep). The glider-measured anomalies (Figures 4a–4f) are averaged along the inshore 200 km of lines 66.7 (green), 80 (blue), and 90 (red). NAM model (g) net surface heat flux (positive indicates downward) and (h) wind stress magnitude are averaged over the oceanic domain of Figure 1 ([–128°, –116°W] × [30°, 38°N]), i.e., data above land are excluded from the spatial average. In Figure 4i Oceanic Niño Index, ONI, shows equatorial SST anomalies averaged over the Niño 3.4 region. All spatially averaged anomalies are filtered with a 3 month running mean. The temporal range of the recent anomalous period is shaded in grey.

Along-isopycnal salinity showed a fresh anomaly during 2014–2015 (Figure 4d). This freshening is caused by the onshore displacement of the relatively fresh offshore waters of the California Current. Consistent with the observed downwelling anomaly (Figures 3 and 4c), we speculate that the onshore displacement resulted from a weakening of the overturning coastal upwelling cell [Davis, 2010]. The negative salinity anomaly on an isopycnal is necessarily accompanied by a negative temperature anomaly; however, this cooling is much weaker than the warming caused by anomalous downwelling (Figure 3b). Alongshore currents (Figure 4e) are dominated by mesoscale variability and do not show a coherent poleward nor equatorward anomaly. Examining salinity on isopycnals allows inference of the integrative effects of advection, while local currents indicate only what advection is at that time. In this case, the onshore displacement of the California Current is revealed by isopycnal salinity analysis.

3.2. Atmospheric Forcing

The net surface heat flux (sum of shortwave radiation, longwave radiation, sensible heat flux, and latent heat flux) anomaly was positive (downward) during most of 2014 (Figure 4g). Of the four heat flux constituents, the shortwave radiation component dominates regional net surface heat flux. Along the Southern California

coast, warm ocean SSTs can impede cloud formation [Schwartz *et al.*, 2014] and reduce cloudiness, which in turn increases downward radiation and surface temperatures [Iacobellis and Cayan, 2013]. This positive feedback likely contributed to the anomalously warm SSTs, high heat content (Figure 4a), and strong stratification (Figure 4b).

Contemporaneous wind stress was weaker than normal. Typically, the winds over the SCCS are alongshore and southward [Nelson, 1977], driving coastal upwelling [Huyer, 1983] and mixing, both of which have cooling effects on the upper ocean. During 2014–2015, the wind stress magnitude was anomalously low (Figure 4h). As reflected in the depressed thermocline (Figure 4c) and high stratification (Figure 4b), the stagnant wind field affected the warm surface pool by reducing upwelling and mixing.

3.3. Other Mechanisms

The evidence argues against anomalous northward advection of warm, southerly water masses. Anomalous alongshore heat advection could be caused by a strengthening and broadening of the California Undercurrent, remote changes of the southerly source water, or a combination of the two. Intensification of the California Undercurrent brings more warm water into the SCCS region and may be evident in velocity or volume transport. Neither alongshore velocity (Figure 4e) nor volume transport was unusual during 2014–2015. Remote warming anomalies in the southerly water masses are advected into the region via the California Undercurrent regardless of local flow anomalies and are detectable through the arrival of positive temperature and salinity anomalies on isopycnals. Along-isopycnal temperature and salinity did not show positive anomalies during 2014–2015; in fact, isopycnals just below the mixed layer showed a slight cooling and freshening trend (Figure 4d). The warming cannot be attributed to horizontal advective influences from the south.

Coastally trapped waves are a possible forcing mechanism. However, given the 2–3 weeks between glider sections and coastally trapped wave speeds that imply a roughly 2 day travel time between lines 90 and 66.7 [Todd *et al.*, 2011a], our data were not sufficient to evaluate this mechanism. Tide gauge [Enfield and Allen, 1980; Chelton and Davis, 1982] and/or satellite observations [Strub and James, 2002] of sea surface height would be required to resolve the influence of coastally trapped waves, but the analysis of those data sets is beyond the scope of our study. While we do not eliminate coastally trapped waves as a possible forcing mechanism, we do note that equatorial conditions were near neutral at the onset of the SCCS warming (Figure 4i), making questionable the remote generation of coastally trapped waves. Furthermore, the Gulf of California acts as a barrier to their northward propagation [Strub and James, 2002].

3.4. Biology

The aforementioned physical anomalies in the upper ocean (Figures 4a–4c) generated a biological response. Like the thermocline depth, the nearshore depth of the chl *a* fluorescence maximum was anomalously deep during 2014 along all lines but particularly in the Southern California Bight along line 90 (Figure 4f). In the SCCS, vertical profiles of coastal chl *a* exhibit subsurface maxima just above the nutricline and at the base of the euphotic zone [Cullen and Eppley, 1981; Cullen, 1982]. The same upwelling processes that maintain thermocline shoaling also maintain nutricline shoaling [Hayward and Venrick, 1998]. Thus, the downwelling anomaly of 2014–2015 deepened the nutricline, decreased nutrient enrichment of the euphotic zone, and, consequently, caused the downward displacement of the chl *a* fluorescence maximum (Figure 4f). Moreover, by decreasing nutrient concentration in the source water for mixing and the strength of wind-induced turbulent mixing itself [Cullen, 2015], weak winds (Figure 4h) can cause a reduction in vertical nutrient fluxes [Lewis *et al.*, 1986] to the depleted euphotic zone. Linkages between large-scale chl *a* concentration and wind pattern fluctuations have previously been observed [Venrick *et al.*, 1987; Polovina *et al.*, 1994]. According to previous studies, the depth of the subsurface chl *a* maximum (SCM) is inversely proportional to the concentration of chl *a* at the SCM, the depth-integrated chlorophyll [Herbland and Voituriez, 1979; Mignot *et al.*, 2011; Cullen, 2015], and phytoplankton size and diversity [Chisholm, 1992]. A deepening of the chl *a* maximum suggests a decreased phytoplankton biomass and a shift in community structure toward smaller phytoplankton [Chisholm, 1992; Cermeno *et al.*, 2008; Cullen, 2015], which have bottom-up effects on food and energy availability at higher trophic levels. Since our glider-based measurements do not allow for the evaluation of absolute phytoplankton abundance or size fractionation, these biological consequences of a vertically displaced SCM are inferred based on other published studies.

4. Conclusion

In summary, our observations show that the regional 2014–2015 warming in the SCCS was predominately due to anomalous atmospheric forcing, a combination of high downward heat flux and weak winds. Higher than normal surface heat flux created a warm, highly stratified upper ocean. Weak winds led to weak upwelling and mixing strengths, which reinforced the surface-intensified temperature anomaly. Under normal wind conditions, upwelling of cold water and turbulent mixing would act to decrease the upper ocean heat content. For instance, during 2013 the SCCS region was characterized by anomalously high surface heat flux (Figure 4g) but normal to strong wind stress magnitudes (Figure 4h), which resulted in neutral upper ocean temperatures (Figure 4a). The unique co-occurrence of atmospheric anomalies generated and perpetuated the observed shallow pool of warm water.

While some aspects of the 2014–2015 warm, downwelling anomalies in the SCCS resemble the remote effects of El Niño previously observed on the California coast, the strong surface heat flux and lack of northward advection distinguish the recent forcing mechanisms from those of some previous El Niño events. During El Niño, atmospheric teleconnections can induce low SLP over the coastal SCCS and the primary local atmospheric forcing anomaly is downwelling favorable wind [Schwing *et al.*, 2002], which deepens the thermocline [Chelton and Davis, 1982; Lynn and Bograd, 2002] and generates a subsurface warming [Dever and Winant, 2002; Todd *et al.*, 2011a]. In contrast, the recent warming was strongest near the surface because weak winds (Figure 4h) and downwelling anomalies (Figure 4c) coincided with additional heat input from anomalous downward surface heat flux (Figure 4g). Differences between the subsurface and surface-intensified warming signatures of the 2009–2010 El Niño and the 2014–2015 event, respectively, are apparent in Figure 3a.

Furthermore, local changes were not in phase with conditions at the equator. As indicated by the Oceanic Niño Index (ONI), equatorial SST anomalies remained negative to neutral from January to October 2014 (Figure 4i). SCCS and equatorial temperature anomalies were uncorrelated; in fact, glider-derived temperature anomalies (Figure 4a) preceded the ONI (Figure 4i) in 2014. This suggests a decoupling of tropical and coastal subtropical dynamics. As of July 2015, the equatorial Pacific is exhibiting El Niño conditions, characterized by a positive ONI of 0.5°C or greater, and the NOAA Climate Prediction Center is forecasting a continuation of El Niño in the Northern Hemisphere through winter 2015–2016 with 95% certainty. The recent development of equatorial El Niño conditions lags the start of the 2014–2015 North Pacific warming by more than a year.

Though it was not directly driven by equatorial dynamics, the 2014–2015 warming in the SCCS was likely connected to large-scale perturbation patterns in the North Pacific. Wind and surface heat flux anomalies were observed in the northeast [Bond *et al.*, 2015; Hartmann, 2015] and other regions of the Pacific, suggesting possible atmospheric teleconnections between remote areas of the basin. Regional atmospheric and oceanic anomalies evolved concurrently (Figure 4), exhibiting the coastal effects of basin-wide climate variability.

The 2014–2015 physical anomalies forced a biological response in the vertical distribution, and possibly the abundance, of chl *a* fluorescence. Such changes at the base of the food web could have ecosystem-wide implications. At higher trophic levels, observed biological anomalies in early 2015 included the mass stranding and high mortality rates of red tuna crabs (*Pleuroncodes planipes*) and California sea lion (*Zalophus californianus*) pups. While the peak of the recent warming has passed, regional oceanic properties remain anomalous relative to climatological conditions. With a strong El Niño event in the forecast for winter 2015–2016, the evolution of the SCCS surface-intensified warm pool remains to be seen.

References

- Alexander, M. A., I. Blade, M. Newman, J. R. Lanzante, N. C. Lau, and J. D. Scott (2002), The atmospheric bridge: The influence of ENSO teleconnections on air-sea interaction over the global oceans, *J. Clim.*, *15*(16), 2205–2231, doi:10.1175/1520-0442(2002)015<2205:Tabtio>2.0.Co;2.
- Beardsley, R. C., E. P. Dever, S. J. Lentz, and J. P. Dean (1998), Surface heat flux variability over the northern California shelf, *J. Geophys. Res.*, *103*(C10), 21,553–21,586, doi:10.1029/98JC01458.
- Bograd, S. J., and R. J. Lynn (2003), Long-term variability in the Southern California Current System, *Deep Sea Res., Part II*, *50*(14–16), 2355–2370, doi:10.1016/s0967-0645(03)00131-0.
- Bograd, S. J., T. K. Chereskin, and D. Roemmich (2001), Transport of mass, heat, salt, and nutrients in the Southern California Current System: Annual cycle and interannual variability, *J. Geophys. Res.*, *106*(C5), 9255–9275, doi:10.1029/1999JC000165.
- Bond, N. A., M. F. Cronin, H. Freeland, and N. Mantua (2015), Causes and impacts of the 2014 warm anomaly in the NE Pacific, *Geophys. Res. Lett.*, *42*, 3414–3420, doi:10.1002/2015GL063306.
- Bretherton, F. P., R. E. Davis, and C. B. Fandry (1976), Technique for objective analysis and design of oceanographic experiments applied to MODE-73, *Deep-Sea Res.*, *23*(7), 559–582, doi:10.1016/0011-7471(76)90001-2.

Acknowledgments

We thank Russ Davis for initiating the California Underwater Glider Network. The Scripps Institution of Oceanography Instrument Development Group was responsible for glider operations, especially Jeff Sherman, Brent Jones, Evan Randall-Goodwin, and Derek Vana; we are grateful for their professionalism. Sarah Gille and Peter Franks provided beneficial comments. The California Underwater Glider Network is supported by NOAA through the Climate Observation Division and the Consortium for the Ocean's Role in Climate (NA10OAR4320156) and through the Southern California Coastal Ocean Observing System (NA11NOS0120029). Additional salary support was provided by NSF through the Repeat Observations by Gliders in the Equatorial Region project (OCE1232971). Data from the California Underwater Glider Network can be obtained via NOAA ERDDAP (<http://coastwatch.pfeg.noaa.gov/erddap/index.html>). The NOAA Climate Prediction Center (www.cpc.ncep.noaa.gov) and the NOAA National Operational Model Archive and Distribution System (nomads.ncdc.noaa.gov) provide access to the ONI and NAM model, respectively.

- Cermeño, P., S. Dutkiewicz, R. P. Harris, M. Follows, O. Schofield, and P. G. Falkowski (2008), The role of nutricline depth in regulating the ocean carbon cycle, *Proc. Natl. Acad. Sci. U.S.A.*, *105*(51), 20,344–20,349, doi:10.1073/pnas.0811302106.
- Chelton, D. B., and R. E. Davis (1982), Monthly mean sea-level variability along the west coast of North America, *J. Phys. Oceanogr.*, *12*(8), 757–784, doi:10.1175/1520-0485(1982)012<0757:Mmslva>2.0.Co;2.
- Chelton, D. B., M. G. Schlax, M. H. Freilich, and R. F. Milliff (2004), Satellite measurements reveal persistent small-scale features in ocean winds, *Science*, *303*(5660), 978–983, doi:10.1126/science.1091901.
- Chisholm, S. W. (1992), Phytoplankton size, *Environ. Sci. Res.*, *43*, 213–237.
- Cullen, J. J. (1982), The deep chlorophyll maximum: Comparing vertical profiles of chlorophyll-a, *Can. J. Fish. Aquat. Sci.*, *39*(5), 791–803, doi:10.1139/f82-108.
- Cullen, J. J. (2015), Subsurface chlorophyll maximum layers: Enduring enigma or mystery solved?, *Annu. Rev. Mar. Sci.*, *7*, 207–239, doi:10.1146/annurev-marine-010213-135111.
- Cullen, J. J., and R. W. Eppley (1981), Chlorophyll maximum layers of the Southern California Bight and possible mechanisms of their formation and maintenance, *Oceanol. Acta*, *4*(1), 23–32.
- Davis, R. E. (2010), On the coastal-upwelling overturning cell, *J. Mar. Res.*, *68*(3–4), 369–385, doi:10.1357/002224010794657173.
- Davis, R. E., M. D. Ohman, D. L. Rudnick, J. T. Sherman, and B. Hodges (2008), Glider surveillance of physics and biology in the Southern California Current system, *Limnol. Oceanogr.*, *53*(5), 2151–2168.
- Dever, E. P., and C. D. Winant (2002), The evolution and depth structure of shelf and slope temperatures and velocities during the 1997–1998 El Niño near Point Conception, California, *Prog. Oceanogr.*, *54*(1–4), 77–103, doi:10.1016/S0079-6611(02)00044-7.
- Di Lorenzo, E., A. J. Miller, N. Schneider, and J. C. McWilliams (2005), The warming of the California Current System: Dynamics and ecosystem implications, *J. Phys. Oceanogr.*, *35*(3), 336–362, doi:10.1175/Jpo-2690.1.
- Di Lorenzo, E., et al. (2008), North Pacific Gyre Oscillation links ocean climate and ecosystem change, *Geophys. Res. Lett.*, *35*, L08607, doi:10.1029/2007GL032838.
- Emery, W. J., and K. Hamilton (1985), Atmospheric forcing of interannual variability in the Northeast Pacific-Ocean—Connections with El Niño, *J. Geophys. Res.*, *90*(Nc1), 857–868, doi:10.1029/JC090iC01p00857.
- Enfield, D. B., and J. S. Allen (1980), On the structure and dynamics of monthly mean sea-level anomalies along the Pacific coast of North and South America, *J. Phys. Oceanogr.*, *10*(4), 557–578, doi:10.1175/1520-0485(1980)010<0557:Otsado>2.0.Co;2.
- Hartmann, D. L. (2015), Pacific sea surface temperature and the winter of 2014, *Geophys. Res. Lett.*, *42*, 1894–1902, doi:10.1002/2015GL063083.
- Hayward, T. L., and E. L. Venrick (1998), Nearsurface pattern in the California Current: Coupling between physical and biological structure, *Deep Sea Res., Part II*, *45*(8–9), 1617–1638, doi:10.1016/S0967-0645(98)80010-6.
- Herbland, A., and B. Voituriez (1979), Hydrological structure-analysis for estimating the primary production in the tropical Atlantic Ocean, *J. Mar. Res.*, *37*(1), 87–101.
- Huyer, A. (1983), Coastal upwelling in the California Current System, *Prog. Oceanogr.*, *12*, 259–284.
- Iacobellis, S. F., and D. R. Cayan (2013), The variability of California summertime marine stratus: Impacts on surface air temperatures, *J. Geophys. Res. Atmos.*, *118*, 9105–9122, doi:10.1002/jgrd.50652.
- Lewis, M. R., W. G. Harrison, N. S. Oakey, D. Hebert, and T. Platt (1986), Vertical nitrate fluxes in the oligotrophic ocean, *Science*, *234*(4778), 870–873, doi:10.1126/science.234.4778.870.
- Lynn, R. J., and S. J. Bograd (2002), Dynamic evolution of the 1997–1998 El Niño-La Niña cycle in the Southern California Current System, *Prog. Oceanogr.*, *54*, 59–75.
- Lynn, R. J., and J. J. Simpson (1987), The California Current System—The seasonal variability of its physical characteristics, *J. Geophys. Res.*, *92*(C12), 12,947–12,966, doi:10.1029/JC092iC12p12947.
- Lynn, R. J., and J. J. Simpson (1990), The flow of the undercurrent over the continental borderland off Southern California, *J. Geophys. Res.*, *95*(C8), 12,995–13,008, doi:10.1029/JC095iC08p12995.
- Mantua, N. J., S. R. Hare, Y. Zhang, J. M. Wallace, and R. C. Francis (1997), A Pacific interdecadal climate oscillation with impacts on salmon production, *Bull. Am. Meteorol. Soc.*, *78*(6), 1069–1079.
- McPhaden, M. J. (1999), Genesis and evolution of the 1997–98 El Niño, *Science*, *283*(5404), 950–954, doi:10.1126/science.283.5404.950.
- Meyers, S. D., A. Melsom, G. T. Mitchum, and J. J. O'Brien (1998), Detection of the fast Kelvin wave teleconnection due to El Niño Southern Oscillation, *J. Geophys. Res.*, *103*(C12), 27,655–27,663, doi:10.1029/98JC02402.
- Mignot, A., H. Claustre, F. D'Ortenzio, X. Xing, A. Poteau, and J. Ras (2011), From the shape of the vertical profile of in vivo fluorescence to chlorophyll-a concentration, *Biogeosciences*, *8*(8), 2391–2406, doi:10.5194/bg-8-2391-2011.
- Miller, A. J., D. R. Cayan, T. P. Barnett, N. E. Graham, and J. M. Oberhuber (1994), Interdecadal variability of the Pacific-Ocean—Model response to observed heat-flux and wind stress anomalies, *Clim. Dyn.*, *9*(6), 287–302, doi:10.1007/Bf00204744.
- Nelson, C. S. (1977), Wind stress and wind stress curl over the California Current Rep National Oceanic and Atmospheric Administration, NOAA Tech. Rep. NMFS SSRF-714.
- Polovina, J. J., G. T. Mitchum, N. E. Graham, M. P. Craig, E. E. Demartini, and E. Flint (1994), Physical and biological consequences of a climate event in the central North Pacific, *Fish. Oceanogr.*, *3*(1), 15–21.
- Ramp, S. R., J. L. McClean, C. A. Collins, A. J. Semtner, and K. A. S. Hays (1997), Observations and modeling of the 1991–1992 El Niño signal off central California, *J. Geophys. Res.*, *102*(C3), 5553–5582, doi:10.1029/96JC03050.
- Roemmich, D., and J. McGowan (1995), Climatic warming and the decline of zooplankton in the California Current, *Science*, *267*(5202), 1324–1326, doi:10.1126/science.267.5202.1324.
- Rudnick, D. L., and S. T. Cole (2011), On sampling the ocean using underwater gliders, *J. Geophys. Res.*, *116*, C08010, doi:10.1029/2010JC006849.
- Rudnick, D. L., R. E. Davis, C. C. Eriksen, D. M. Fratantoni, and M. J. Perry (2004), Underwater gliders for ocean research, *Mar. Technol. Soc. J.*, *38*(2), 73–84.
- Schwartz, R. E., A. Gershunov, S. F. Iacobellis, and D. R. Cayan (2014), North American west coast summer low cloudiness: Broad-scale variability associated with sea surface temperature, *Geophys. Res. Lett.*, *41*, 3307–3314, doi:10.1002/2014GL059825.
- Schwing, F. B., T. Murphree, L. deWitt, and P. M. Green (2002), The evolution of oceanic and atmospheric anomalies in the northeast Pacific during the El Niño and La Niña events of 1995–2001, *Prog. Oceanogr.*, *54*(1–4), 459–491, doi:10.1016/S0079-6611(02)00064-2.
- Sherman, J., R. E. Davis, W. B. Owens, and J. Valdes (2001), The autonomous underwater glider "Spray", *IEEE J. Oceanic Eng.*, *26*(4), 437–446.
- Strub, P. T., and C. James (2002), The 1997–1998 oceanic El Niño signal along the southeast and northeast Pacific boundaries—An altimetric view, *Prog. Oceanogr.*, *54*(1–4), 439–458, doi:10.1016/S0079-6611(02)00063-0.
- Todd, R. E., D. L. Rudnick, R. E. Davis, and M. D. Ohman (2011a), Underwater gliders reveal rapid arrival of El Niño effects off California's coast, *Geophys. Res. Lett.*, *38*, L03609, doi:10.1029/2010GL046376.

- Todd, R. E., D. L. Rudnick, M. R. Mazloff, R. E. Davis, and B. D. Cornuelle (2011b), Poleward flows in the Southern California Current System: Glider observations and numerical simulation, *J. Geophys. Res.*, *116*, C02026, doi:10.1029/2010JC006536.
- Venrick, E. L., J. A. McGowan, D. R. Cayan, and T. L. Hayward (1987), Climate and chlorophyll-a—Long-term trends in the central North Pacific Ocean, *Science*, *238*(4823), 70–72, doi:10.1126/science.238.4823.70.
- Wang, S. Y., L. Hipps, R. R. Gillies, and J. H. Yoon (2014), Probable causes of the abnormal ridge accompanying the 2013–2014 California drought: ENSO precursor and anthropogenic warming footprint, *Geophys. Res. Lett.*, *41*, 3220–3226, doi:10.1002/2014GL059748.
- Whitney, F. A. (2015), Anomalous winter winds decrease 2014 transition zone productivity in the NE Pacific, *Geophys. Res. Lett.*, *42*, 428–431, doi:10.1002/2014GL062634.
- Winant, C. D., and C. E. Dorman (1997), Seasonal patterns of surface wind stress and heat flux over the Southern California Bight, *J. Geophys. Res.*, *102*(C3), 5641–5653, doi:10.1029/96JC02801.